



Generation of humidity-sensitive genic male sterility in maize and wheat for hybrid seed production

Xingchen Xiong , Dan Wang, Changfeng Guo , Guiqiang Fan , Yingchun Zhang, Bo Song, Binzhu Hou, Yuanyuan Yan, Chuanxiao Xie , Xiaoduo Lu, Chunyi Zhang and Xiaoquan Qi* 

A two-line system based on environment-sensitive genic male sterility (EGMS) offering controllable fertility is a favorable approach for crop hybrid breeding (Fan and Zhang, 2017). The discovery of humidity-sensitive genic male sterility (HGMS) in rice (*Oryza sativa*) provides a new approach to facilitate hybrid seed production (Peng et al., 2022; Qiao et al., 2023). However, to date, no varieties exhibiting HGMS have been identified in maize (*Zea mays*) or wheat (*Triticum aestivum*).

In our previous study, loss of function of the rice triterpene synthase gene *OXIDOSQUALENE CYCLASE12* (*OsOSC12*, also reported as *POACEATAPETOL SYNTHASE1* (*OsPTS1*)) led to failure of pollen coat formation and the mutants were male sterile at low relative humidity (RH), but fully male fertile at high RH (Xue et al., 2018). Proteins homologous to *OsPTS1* exist in other grass species and are conserved (Xue et al., 2018; Guo et al., 2021). Of these, there are one ortholog, *ZmPTS1* in maize, and there are three homeologs, *TaPTS1-A*, *TaPTS1-B* and *TaPTS1-D*, in wheat. All four genes were specifically expressed in anthers (Figures S1, S2A, B). Here, we report the creation of HGMS lines through knockout of these *PTS1* genes in maize and wheat.

We obtained two independent knockout maize mutants for *ZmPTS1* in the KN5585 background, named *ko-1* (1-bp deletion) and *ko-5* (10-bp deletion), via clustered regularly interspaced small palindromic repeats (CRISPR)/CRISPR-associated nuclease 9-mediated genome editing (Figure 1A). We also screened an ethyl methanesulfonate (EMS)-induced mutant library in the B73 background and identified three mutant lines with amino acid substitutions in *ZmPTS1* (Figure 1A). Of these, we found that the *ZmPTS1*^{D415N} variant harboring the mutation detected in the *d3* mutant is a loss-of-functional enzyme, based on a biochemical analysis using protein produced in the yeast *Pichia pastoris* (Figure S3A, B). Potassium iodide staining showed that pollen from all *Zmpst1* mutants is as viable as the WT pollen (Figure S4A). Notably, fresh pollen grains shed from the anthers of *d3*, *ko-1* and *ko-5* flowers immediately became dehydrated and completely collapsed within 90 s, whereas those from the wild-type (WT) only started to shrink after 5 min, completely collapsing in 2 h (Figures S4B, C, 1B). Furthermore, ultra-thin section examination of the pollen wall revealed that *ko-1*, *ko-5* and *d3* have fewer components in their pollen coat than the WT (Figure 1C), similar to that of HGMS mutant in rice (Xue et al., 2018), suggesting the lack of pollen coat results in rapid dehydration of *Zmpts1* pollen.

To estimate the relationship between dehydrated pollen and its germination, we conducted pollen vitality assays. In an *in vitro* pollen germination assay, fresh pollen from the mutant line *ko-1* and the WT KN5585 had similarly high vitality, with up to a 50% germination rate, at humidity levels of 100% (fluid medium) (Figures S5A, B, 0 min). The germination rates of pollen grains from *ko-1* decreased dramatically after exposure to normal atmospheric conditions (50%–60% RH), dropping to <1% after 2 min of exposure, whereas KN5585 pollen grains retained germination competency even after 90 min (Figure S5A, B, 2 and 90 min). Furthermore, an *in vivo* pollen germination assay on maize silk indicated that pollen grains from the *ko-1* mutant quickly collapse on the dry silk and cannot germinate at RH < 60% (Figure S5C). Thus, we conclude that the pollen grains of mutants not only dehydrate rapidly but also lose their vitality for germination.

Importantly, *ko-1* pollen showed the same capacity for germination as WT pollen when the recipient silks were maintained in an environment with very high RH (>90%) (Figure S5C), providing a convenient and cost-effective method for multiplication of *Zmpts1* mutants. Furthermore, we determined that pollen of the *ko-1* mutant line shows a delay in dehydration as the ambient RH increased and remains fully hydrated for up to 90 min when maintained at ≥90% RH (Figure S6A, B). Therefore, two approaches were used for maintaining pollen vitality to ensure self-pollination of *Zmpts1* mutants. First, we sprayed water directly onto the silks, followed by artificial (hand) pollination (Figure 1D, method1). Second, we increased and maintained the local RH to high levels around maize ears and silks by generating a fog layer via spraying water using a high-pressure sprayer during the pollen dispersal period (Figure 1D, method2). Both methods restored the fertility of the *ko-1* mutant line, leading to high seed-setting rates for maize HGMS lines (Figure 1E).

To evaluate the seed-setting performance of the *Zmpts1* mutants in the field, we conducted multi-year field experiments in Beijing, Lingshui (Hainan Province) and Zepu (Xinjiang Uyghur Autonomous Region), China. The seed-setting rates of *d3*, *ko-1* and *ko-5* were between 0% and 3%, with average values not exceeding 1% (Figure 1F, G), indicating that the *Zmpts1* mutants have stable and severe sterility across variable humidity conditions (Figure S7A–F). To elucidate why the *Zmpts1* mutant lines consistently exhibit stable and exceptionally low seed-setting rates even in

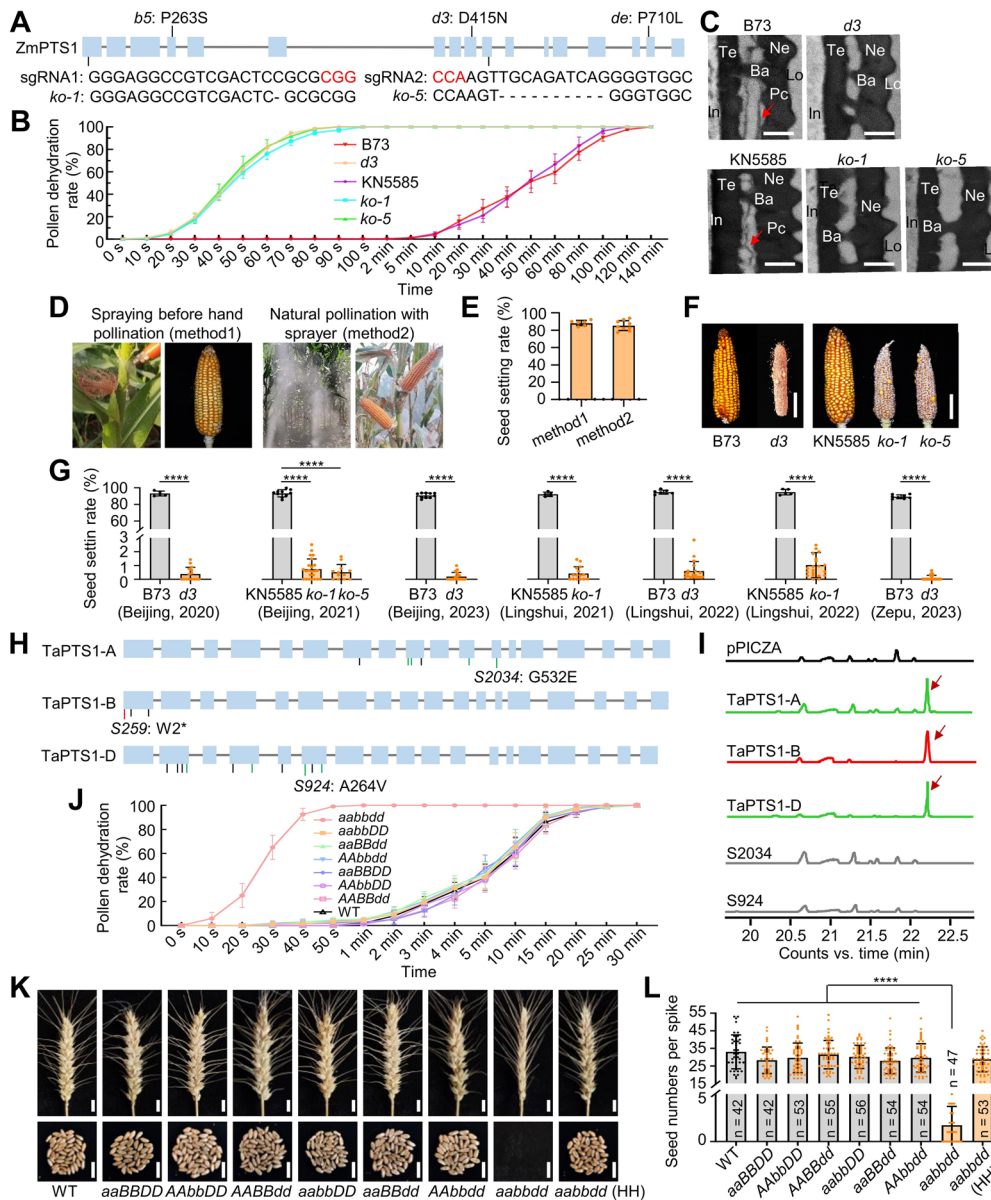


Figure 1. Creation of humidity-sensitive genic male-sterile (HGMS) lines in maize and wheat

(A) Diagram of the *ZmPTS1* locus showing the mutations in *ZmPTS1*. Blue boxes represent exons. The three ethyl methanesulfonate (EMS)-induced mutations identified in the B73 inbred lines are shown above; the positions of the two single guide RNAs used to generate knockout mutants in the KN5585 background are shown below, with the wild-type (WT) and mutant sequences at each target site. **(B)** Pollen dehydration analysis over time at 26°C–28°C and 40%–60% relative humidity (RH). The percentages of dehydrated pollen at each time point are shown, as means \pm SD. **(C)** Transmission electron microscopy analysis of ultra-thin sections of mature pollen wall from WT and mutants. Ba, bacula; In, intine; Lo, locule; Ne, nexine; Pc, pollen coat (red arrows); Te, tectum. Scale bars, 0.5 μ m. **(D)** Effect of spraying water before hand-pollination and natural pollination with sprayer. The sprayer was active for 5 min then stopped for 10 min, for 7 h every day during flowering. The left panels show the humidification method; the right panels show the corresponding ears ready for harvesting. **(E)** Seed-setting rate of *ko-1* pollinated by each humidification method. Values are means \pm SD. **(F)** Representative ears from the WT and mutants grown in the field. Scale bars, 4.5 cm. **(G)** Seed-setting rates for WT and mutant ears harvested in different geographical areas and different years. Values are mean \pm SD; a two-tailed Student's *t*-test was used to determine the *P*-values; *****P* < 0.0001. **(H)** Diagrams of gene structure and position of mutations for TaPTS1-A, TaPTS1-B and TaPTS1-D in wheat. Blue boxes represent exons. Nan3-induced mutations responsible for amino acid substitutions in the Xichang 76-9 background are shown below, with green vertical lines indicating mutants retaining biochemical function; the red vertical line indicates a stop codon. S2034, S259 and S924 represent loss-of-function mutants crossed to obtain double and triple mutants (Tapts1aabbdd). **(I)** Gas chromatography–mass spectrometry (GC–MS) profiles for WT and mutant TaPTS1 proteins produced in *Pichia pastoris*. Red arrows indicate the extracted-ion chromatogram for catalytic products. pPICZA, empty vector. **(J)** Pollen dehydration analysis over time at 23°C–28°C and 40%–55% RH, shown as a percentage of dehydrated pollen, with means \pm SD. **(K)** Representative photographs of spikes (top) and grains (bottom) harvested from WT and mutants under natural conditions. HH, high humidity; scale bars, 1.25 cm. **(L)** Seed number per spike for WT and mutants under natural conditions in Beijing, 2023. Values are means \pm SD; a two-tailed Student's *t*-test was used to determine the *P*-values; *****P* < 0.0001.

environments with very high RH, we examined the anther dehiscence process across various RH conditions (Figure S8A, B). Our observations revealed that anther dehiscence fails under extremely high RH or during rainy conditions. This phenomenon has been previously documented and is considered advantageous for pollen dispersal and the preservation of pollen viability (Kerner von Marilaun, 1895; Joan and Jordan, 1992; Humphreys and Skema, 2023).

To explore the possibility of hybrid seed production in the field via HGMS in maize, we grew the EMS-induced *Zmpts1* mutant *d3* plants with other maize inbred lines in field plots in Zhangye, Gansu Province, a major area of maize hybrid seed production in China. In this experiment, we grew more than 100 *d3* plants and used them as female parents to receive pollen from other inbred lines planted nearby (Figure S9A). Notably, we obtained an average seed-setting rate of 85%, the same as that with traditional hybrid seed production (Figure S9B). The vast majority (>99%) of the *d3* ear progeny were heterozygous for the *ZmPTS1*^{D415N} mutation, based on the genotyping of 1,362 kernels from 15 randomly selected ears (Figure S9C; Table S1). This hybrid seed purity exceeds the requirements of the maize seed industry production. In addition, we observed no negative effects on agronomic traits in the *Zmpts1* mutants compared to the corresponding WT plants (Figure S10A–I). Taken together, our results demonstrate that the two-line system based on HGMS is a convenient and cost-effective approach for hybrid maize breeding and large-scale hybrid seed production.

Meanwhile, we carried out a screening of NaN₃-induced wheat mutations in each *TaPTS1* gene from the Xichang 76-9 mutant library, yielding 6, 3 and 10 mutations resulting in amino acid substitutions in *TaPTS1-A*, *TaPTS1-B* and *TaPTS1-D*, respectively (Figure 1H). Among these, S259 has a premature stop codon in *TaPTS1-B* and is likely to be a *TaPTS1-B* mutant. To identify which *TaPTS1-A* and *TaPTS1-D* mutants lead to a nonfunctional enzyme, we carried out an enzymatic assay in *P. pastoris*. The *TaPTS1-A*^{G532E} and *TaPTS1-D*^{A264V} proteins showed no catalytic activity when expressed in *P. pastoris*, indicating that S2034 and S924 are *TaPTS1-A* and *TaPTS1-D* mutants, respectively (Figures 1I, S11A–C). We crossed the three loss-of-function mutants of *TaPTS1-A*, *TaPTS1-B* and *TaPTS1-D*, starting with a S259 × S924 cross to obtain F₁ progeny, which we then crossed to S2034 to obtain the triple mutant (hereafter *aabbdd*). The pollen of all single and double mutants dehydrated slowly and had the same high fertility as the WT pollen, whereas the pollen of the triple mutant dehydrated quickly and collapsed completely within 1 min (Figures 1J, S12B), suggesting that *TaPTS1-A*, *TaPTS1-B* and *TaPTS1-D* are functionally redundant. In field experiments, the *aabbdd* line exhibited male sterility or a decreased seed-setting rate, but its fertility was restored at high RH (Figures 1K, L, S13A–E). We observed no other negative traits in *TaPTS1aabbdd* mutant lines (Figure S14A–C). The created wheat HGMS lines constitute highly desirable materials for hybrid breeding and heterosis utilization in wheat.

Maize and wheat humidity-sensitive genic male sterility

In summary, we generated HGMS lines in the two major cereal crops, maize and wheat, based on mutations in the respective *PTS1* genes and demonstrated that a two-line hybrid seed production system based on these HGMS lines is a convenient and cost-effective approach for effective utilization of maize heterosis.

ACKNOWLEDGEMENTS

We are grateful to Ms. Hui Han of Zhangye Denghai Seed Industry Co., Ltd. for her assistance in designing our field experiment for hybrid seed production. This work was funded by the National Key Research and Development of China (2022YFF1003504), the National Natural Science Foundation of China (32101769, 31530050), the Strategic Priority Research Program of the Chinese Academy of Sciences (XDA26030301).

CONFLICTS OF INTEREST

The authors declare no conflict of interest.

AUTHOR CONTRIBUTIONS

X.Q. conceived the project. X.X. and X.Q. wrote the manuscript. X.X., D.W., C.G., G.F., Y.Z., B.S. and B.H. performed the experiments. Y.Y. and C.X. generated maize gene-editing mutants. X.L. and C.Z. provided maize EMS-mutagenesis materials. All authors read and approved of its content.

Xingchen Xiong^{1,2,3} , Dan Wang^{1,2,3},
Changfeng Guo^{1,2,3} , Guiqiang Fan⁴ ,
Yingchun Zhang^{1,2}, Bo Song^{1,2}, Binzhu Hou^{1,2},
Yuanyuan Yan⁵, Chuanxiao Xie⁵ , Xiaoduo Lu⁶,
Chunyi Zhang⁷ and Xiaoquan Qi^{1,2*} 

1. Key Laboratory of Plant Molecular Physiology, Institute of Botany, The Chinese Academy of Sciences, Beijing 100093, China
2. China National Botanical Garden, Beijing 100093, China
3. University of Chinese Academy of Sciences, Beijing 100049, China
4. Institute of Grain Crops, Xinjiang Academy of Agricultural Sciences, Urumchi 830091, China
5. Institute of Crop Science, Chinese Academy of Agricultural Sciences, Beijing 100081, China
6. Institute of Molecular Breeding for Maize, Qilu Normal University, Jinan 250200, China
7. Biotechnology Research Institute, Chinese Academy of Agricultural Sciences, Beijing 100081, China

*Correspondence: Xiaoquan Qi (xqi@ibcas.ac.cn)

Edited by: Lin Li, Huazhong Agricultural University, China

Received Jun. 24, 2024; Accepted Jul. 30, 2024

Xue, Z., Xu, X., Zhou, Y., Wang, X., Zhang, Y., Liu, D., Zhao, B., Duan, L., and Qi, X. (2018). Deficiency of a triterpene pathway results in humidity-sensitive genic male sterility in rice. *Nat. Commun.* **9**: 604.

REFERENCES

- Fan, Y., and Zhang, Q. (2017). Genetic and molecular characterization of photoperiod and thermo-sensitive male sterility in rice. *Plant Reprod.* **31**: 3–14.
- Guo, C., Xiong, X., Dong, H., and Qi, X. (2021). Genome-wide investigation and transcriptional profiling of the oxidosqualene cyclase (OSC) genes in wheat (*Triticum aestivum*). *J. Syst. Evol.* **60**: 1378–1392.
- Humphreys, E.A., and Skema, C. (2023). Just add water: Rainfall-induced anther closure and color change in *Ripariosida hermaphrodita* (Malvaceae). *Ecol. Evol.* **13**: e10219.
- Joan, E., and Jordan, J.R. (1992). Reversible anther opening in *Lilium philadelphicum* (Liliaceae): A possible means of enhancing male fitness. *Am. J. Bot.* **79**: 144–148.
- Kerner von Marilaun, A. (1895). *The natural history of plants: their forms, growth, reproduction, and distribution. Half-volume III.* Translated by Oliver, F., Busk, M., Macdonald, M. Henry Holt, Co., New York.
- Peng, G., Liu, Z., Zhuang, C., and Zhou, H. (2022). Environment-sensitive genic male sterility in rice and other plants. *Plant Cell Environ.* **46**: 1120–1142.
- Qiao, Y., Hou, B., and Qi, X. (2023). Biosynthesis and transport of pollen coat precursors in angiosperms. *Nat. Plants* **9**: 864–876.

SUPPORTING INFORMATION

Additional Supporting Information may be found online in the supporting information tab for this article: <http://onlinelibrary.wiley.com/doi/10.1111/jipb.13768/supinfo>

- Figure S1.** Relative expression levels of *ZmPTS1* in different maize tissues
- Figure S2.** Expression pattern of *TaPTS1-A*, *TaPTS1-B* and *TaPTS1-D*
- Figure S3.** Biochemical functional identification of wild-type (WT) and mutant *ZmPTS1* in *Pichia pastoris*
- Figure S4.** Microscopy analysis of pollen dehydration in maize
- Figure S5.** Analysis of pollen viability and anther dehiscence
- Figure S6.** Delay pollen dehydration of *Zmpts1* mutants by humidity
- Figure S7.** Daily humidity records during the dispersal period of mutant pollen in the field
- Figure S8.** The relationship of anther dehiscence and humidity
- Figure S9.** Confirmation of hybrid seed production in maize
- Figure S10.** Analysis of agronomic traits for wild-type (WT) and mutants
- Figure S11.** Functional identification of *Tapts1-a* and *Tapts1-d* mutants
- Figure S12.** Pollen vitality and dehydration analysis in wheat
- Figure S13.** Methods of fertility restoration and seed-setting analysis
- Figure S14.** Analysis of agronomic traits for wild-type (WT) and mutants
- Table S1.** Purity determination of *d3* for hybrid seed production
- Table S2.** Primers used in the maize study
- Table S3.** Primers used in the wheat study



Scan the QR code to view JIPB on WeChat (WeChat: [jipb1952](#))



Scan the QR code to view JIPB on Twitter (Twitter: [@JIPBio](#))